Inertial self-propulsion of spherical microswimmers by rotation-translation coupling

Itzhak Fouxon[1,2,*] and Yizhar Or[2,†]

[1]*Department of Chemical Engineering, Technion–Israel Institute of Technology, Haifa 3200003, Israel*
[2]*Faculty of Mechanical Engineering, Technion–Israel Institute of Technology, Haifa 3200003, Israel*

(Received 19 November 2017; revised manuscript received 15 October 2018; published 5 February 2019)

We study swimming of small spherical particles that regulate fluid flow on their surface by applying tangential squirming strokes. We derive translational and rotational velocities for any given stroke which is not restricted by axial symmetry as assumed usually. The formulation includes inertia of both the fluid and the swimmer, motivated by inertia's relevance for large *Volvox* colonies. We show that inertial contribution to mean speed comes from dynamic coupling between translation and rotation, which occurs only for strokes that break axial symmetry. Remarkably, this effect enables overcoming the scallop theorem on impossibility of propulsion by time-reversible strokes. We study examples of tangential strokes of an axisymmetric traveling wave and of asymmetric time-reversible flapping. In the latter case, we find that the inertia-driven mean speed is optimized for flapping frequency and the swimmer's size, which fall well within the range of realistic physical values for *Volvox* colonies. We conjecture that similarly to *Paramecia*, large *Volvox* could use time-reversible strokes for inertia-driven swimming coupled with their rotations.

DOI: 10.1103/PhysRevFluids.4.023101

I. INTRODUCTION

Spherical microswimmers are a unique model of swimming at low Reynolds number which is theoretically tractable. Its introduction is motivated by ciliated microorganisms [1,2] as well as flagellated colonies of *Volvox* algae [3,4]. The interaction of these organisms with the fluid is described by no-slip boundary conditions on a nearly spherical time-dependent envelope of the tips of cilia or flagella whose motion is actuated by the swimmer (squirming). This boundary velocity sets the fluid in motion, which applies propulsion force on the swimmer [1–17]. Due to smallness of the Reynolds number, the fluid motion can be described by linear, steady or unsteady, Stokes equations. The linearity and the spherical shape offer the possibility of a detailed solution connecting microscopic motions of the actuated envelope with the swimmer's motion as a whole.

Previous treatments mostly neglected inertias of both the fluid and the swimmer and assumed axially symmetric swimming strokes as in the original formulation [1,2]. This leads to substantial simplifications in the coupled system of the Navier-Stokes equations (NSEs) governing the flow and the Newton equations governing the swimmer's motion. We first consider the neglect of fluid inertia for which the convective and time-derivative terms of the NSE are dropped. The convective term in the equations, giving the flow derivative along the streamline, is negligible since the Reynolds number (defined as the product of the swimmer's size and velocity divided by the kinematic

*itzhak8@gmail.com
†izi@technion.ac.il

viscosity) is less than 0.1 even for largest *Volvox* colonies [10]. In contrast, the neglect of the time-derivative term in the NSE requires careful consideration. If the fluid inertia is negligible, then this term can be discarded and steady Stokes equations of the flow apply [1,2,18,19]. However, this neglect is invalid for the largest *Volvox* colonies of hundreds of microns in size (*Volvox* comes in aggregates of different numbers of cells and has a range of sizes) [3,10]. Indeed, the significance of the inertia of the fluid is determined by the Roshko number $\mathrm{Ro} = \sigma \tau_d$, where σ is the frequency of the periodic stroke and τ_d is the characteristic time of outward viscous diffusion of momentum from the sphere (sometimes Ro is called the oscillatory Reynolds number [6,20]). This time is proportional to the squared radius of the swimmer divided by the kinematic viscosity. Using the experimentally observed value of $\sigma = 203$ rad/s [3], we have $\mathrm{Ro} \sim 1$ for a colony with a radius of 100 μm. This would invalidate the neglect of inertia for *Volvox* since the typical size range is between 1 and 500 μm. In fact, we demonstrate below that it is plausible that the definition of Ro must be multiplied by a numerical factor of $1/9$. Thus it is reasonable that for colonies smaller than 300 μm we can assume $\mathrm{Ro} \ll 1$ (we observe that Ro has a fast quadratic dependence on the radius). For these small colonies the momentum redistributes over the fluid before the swimmer moves the flagella significantly. The flow is then steady Stokes flow determined by the instantaneous position and velocity of the flagella. However, for colonies larger than 300 μm where $\mathrm{Ro} > 1$, momentum diffusion and swimming stroke are coupled nontrivially. This coupling is described by the unsteady time-derivative term in the NSE whose inclusion is necessary. This term introduces memory where the propulsion force is determined not only by an instantaneous stroke but also by its past values [21–24]. Though this sometimes does not influence the time-averaged net propulsion velocity for periodic strokes, it is relevant for nutrient uptake [17] and reaction to external stimuli [25]. It must be stressed here that the 300-μm threshold is only an estimate. A detailed comparison between the theory and the experiment is needed in order to decide which colonies can be considered inertialess and which must be treated as inertial.

The second of the usually made assumptions is the neglect of a swimmer's inertia, implying that the motion occurs at zero force and torque. This is also invalid for large colonies where the timescale of the viscous drag is comparable to the period of the stroke. In fact, the densities of the swimmer and of the fluid are very close, so the relevance of fluid and particle inertias is determined by the same parameter Ro. Finally, the third assumption of the axially symmetric stroke, in the traditional form without the swirl [10], allows us to use the general solution for axially symmetric flow. This assumption includes zero rotation, thus removing the characteristic rotation of *Volvox* that gave it its name. The rotational velocity was included without destroying the symmetry by introducing an axisymmetric swirl component [10]. In this framework there is no coupling between translation and rotation (in sharp contrast with the coupled rotation and translation considered here). Thus, even though introduction of the axisymmetric swirl helps fit the rotational velocity, it does not help fit the translational velocity that is independent of the parameters of the swirl. Consequently, the existing discrepancy between theoretical predictions for the swimming velocity and the data cannot be resolved by the axisymmetric swirl [10]. An axially symmetric stroke also restricts the motion to a straight line, which is not always the case [13]. This stroke can be unsuitable for the description of physical phenomena as in the case of a phototaxis where a complex interaction between rotation and translation regulates the turning of the colony towards a light source [13,26].

The three assumptions considered above can be invalid, either because $\mathrm{Ro} \sim 1$ or because of asymmetry of the strokes. A few previous works relaxed some of the assumptions. Reference [16] studied the limit case of an inertial heavy (called dense in [16]) swimmer in inertialess fluid, disregarding the rotation of a tangential squirmer. In [17] the equation of motion for the translational velocity of an inertial tangential squirmer in inertial flow was developed using the unsteady reciprocal theorem. However, the equation was solved only for the axially symmetric case where neither inertia changes the time-averaged velocity and the motion is pure axial translation without rotation. This results in oscillatory terms that give nonzero transient motion for a maneuver starting from rest, but no net propulsion in the steady state [6]. On the other hand, the stroke symmetry assumption was relaxed in [12–15], where inertial effects were not considered.

In this work we relax all three assumptions above, which are negligible inertias of the fluid and the swimmer and the axisymmetric swimming strokes. These assumptions do not necessarily hold in practice. The Roshko number is not small for large colonies where the net force is nonzero and the stroke can depend on the azimuthal angle as in phototaxis [13,26]. In contrast, we continue using the assumption of small Reynolds number which is satisfied in practice (finite-Reynolds-number corrections become relevant for sizes close to 1 mm [27,28]). To make the arising problem tractable we make a simplifying assumption that the swimming stroke is tangential. This assumption does not hold for *Volvox*, however it could be that the discovered qualitative phenomenon has relevance for motion of the algae. Namely, we demonstrate that the interplay of the fluid and swimmer's inertia with a tangential asymmetric stroke gives a different mechanism of swimming. In particular, it is usually believed that tangential squirmers that maintain a constant spherical shape cannot swim by a time-reversible stroke; the time-averaged velocity is zero [6,16,17]. However, this conclusion was made only for an axially symmetric stroke that involves no rotation. We demonstrate that an asymmetric time-reversible tangential stroke that does involve rotation can generate self-propulsion via nonlinear rotation-translation coupling. The net swimming velocity considered as a function of inertia parameter Ro reduces to zero as $\mathrm{Ro} \to 0$, in accord with the scallop theorem [18]. As we show below, the leading-order term at $\mathrm{Ro} \ll 1$ is proportional to a time-averaged vector product of instantaneous translational and rotational velocities at $\mathrm{Ro} = 0$. This result is independent of the details of the stroke. We present a concrete example of a time-reversible stroke with nonzero average nondimensional propulsion speed at any $\mathrm{Ro} > 0$. The nondimensional speed decays for small and large values of Ro and reaches a maximum at an intermediate value. This value falls within feasible physical values of large *Volvox* colonies. Thus the discovered phenomenon might have relevance for these algae. For a small swimmer size with negligible inertia, our formulas for translational and rotational velocity of an inertial spherical tangential squirmer in inertial fluid in terms of an arbitrary swimming stroke reduce to those of [29] for an inertialess squirmer in inertialess fluid.

We demonstrate that inertia changes the swimming velocity, obtained by neglecting inertia, directly by producing additive correction and indirectly by changing the rotation velocity. The direct contribution has a zero time average. Thus the scallop theorem implies that a swimmer who does not rotate or whose rotation axis is aligned with the translational velocity could not swim by a time-reversible stroke as was found in [6,16,17] by direct calculation. It must be stressed though that translation during one period in these cases can be nonzero. The indirect influence through the rotation can change the net velocity through the nonlinear interplay of the stroke and the spatial rotation (rotation-translation coupling). This makes the motion quite different from the inertialess case and enables overcoming the scallop theorem.

In the next section we demonstrate that insight into the motion can be obtained by separating the flow into the inertialess component due to the swimming stroke and the inertial friction component. The former describes the motion of an inertialess swimmer in inertial fluid and causes the corresponding translational and swimming velocities. The frictional component describes that, due to inertia, the swimmer has finite (frequency-dependent) relaxation times and lags behind the velocity of the inertialess component.

II. FLOW AS THE SUM OF INERTIALESS SWIMMING AND INERTIAL COMPONENTS

In this section we introduce decomposition of the flow. One component of the flow describes the result of force- and torque-free swimming of an inertialess swimmer in inertial fluid. This flow is of separate interest. The other component describes the propulsion force (and torque) that acts to produce frequency-dependent relaxation of the swimmer's velocity to the velocity of the inertialess swimmer.

We consider tangential squirmers that have the constant shape of a sphere with radius a. The swimming stroke produces in the body-fixed coordinate frame a purely tangential motion of the spherical surface at velocity $\boldsymbol{v}_b(\boldsymbol{x}, t)$. Thus, at time t the velocity of the material point whose coordinate in the body-fixed frame is $\boldsymbol{x}$ is $\boldsymbol{v}_b(\boldsymbol{x}, t)$, where the domain of definition of $\boldsymbol{v}_b$ is $|\boldsymbol{x}| = a$ and

$\boldsymbol{x}\cdot\boldsymbol{v}_b(\boldsymbol{x})=0$. Here, in parallel with assumptions of *Volvox* modeling [3], we assume that the fluid does not change the flagella motion and $\boldsymbol{v}_b(\boldsymbol{x},t)$ is a given quantity determined by the biology of the organism. We stress that $\boldsymbol{v}_b(\boldsymbol{x},t)$ is Eulerian and not a Lagrangian flow field. In the often-used (cf. [1,10]) Lagrangian description, one would describe the swimming stroke by running coordinates of material points $\theta(t)=\theta_0+f_1(\theta_0,\phi_0,t)$ and $\phi(t)=\phi_0+f_2(\theta_0,\phi_0,t)$, where $f_i(\theta_0,\phi_0,t)$ are given (small) functions characterizing the strokes as displacement fields of material points. Here θ_0 and ϕ_0 are initial positions of the point on the sphere as in the usual Lagrangian description of the motion of the fluid [24]. The velocity $\boldsymbol{v}_b(\boldsymbol{x},t)$ is implicitly given by

$$\boldsymbol{v}_b(\theta_0+f_1,\phi_0+f_2,t)=a\hat{\boldsymbol{\theta}}\partial_t f_1+a\sin(\theta_0+f_1)\hat{\boldsymbol{\phi}}\partial_t f_2, \tag{1}$$

where $\hat{\boldsymbol{\theta}}$ and $\hat{\boldsymbol{\phi}}$ are unit vectors in the directions of growth of polar and azimuthal angles, respectively. Solving the equation for all θ_0 and ϕ_0, one can find $\boldsymbol{v}_b(\boldsymbol{x},t)$ in terms of f_i (in practice this involves expansion in the smallness of f_i; see, e.g., [29]). Since both $\boldsymbol{v}_b$ and f_i are determined by the stroke kinematics and not by the interaction with the fluid we consider them as equivalent descriptions which are assumed as given. Thus we will provide swimming velocities in terms of $\boldsymbol{v}_b(\boldsymbol{x},t)$, which can then be rewritten in terms of f_i by solving Eq. (1).

We now consider the description of the stroke in the rest frame of the fluid. The fluid frame coordinate of a material point with body-fixed coordinate $\boldsymbol{x}_b$ can be written as $\boldsymbol{x}_0(t)+\boldsymbol{R}(t)\boldsymbol{x}_b$. Here $\boldsymbol{x}_0(t)$ is the position of the swimmer's center in the frame of the fluid and the rotation matrix $\boldsymbol{R}(t)$ is orthogonal (the axes of the two frames can be made to coincide by translation of the origin and rotation). For definiteness we assume that at $t=0$ the frames coincide so that $\boldsymbol{x}_0(0)=0$ and $R_{ij}(0)=\delta_{ij}$. The equation of the time derivative of the orthogonal matrix $\boldsymbol{R}(t)$ has the general form $\dot{R}_{ij}=\epsilon_{ikl}\Omega_k R_{lj}$, which defines the angular velocity vector $\boldsymbol{\Omega}$. Using $\boldsymbol{\Omega}$ and the center velocity $\boldsymbol{v}=d\boldsymbol{x}_0/dt$, we can write the fluid frame velocity of the material point with coordinate $\boldsymbol{x}_0(t)+\boldsymbol{x}$, where $|\boldsymbol{x}|=a$. This is given by the time derivative of $\boldsymbol{x}_0(t)+\boldsymbol{R}(t)\boldsymbol{x}_b$ that equals $\boldsymbol{v}+\boldsymbol{\Omega}\times\boldsymbol{x}+\boldsymbol{R}\boldsymbol{v}_b(\boldsymbol{R}^{\mathsf{T}}\boldsymbol{x},t)$. This defines the no-slip boundary condition for the fluid flow $\boldsymbol{u}(\boldsymbol{x}-\boldsymbol{x}_0(t),t)$ that we count from the center of the swimmer. Using the assumption that the Reynolds number is small, we find that the flow $\boldsymbol{u}(\boldsymbol{x},t)$ obeys unsteady Stokes equations

$$\partial_t\boldsymbol{u}=-\boldsymbol{\nabla}p+\nu\nabla^2\boldsymbol{u},\quad \boldsymbol{\nabla}\cdot\boldsymbol{u}=0,\quad \boldsymbol{u}(\infty)=0, \tag{2}$$

where p is the pressure (minus the hydrostatic pressure) divided by the fluid density ρ and ν is the fluid kinematic viscosity [30]. The boundary conditions are vanishing for the flow at infinity and

$$\boldsymbol{u}(|\boldsymbol{x}|=a)=\boldsymbol{v}+\boldsymbol{\Omega}\times\boldsymbol{x}+\boldsymbol{u}_b(\boldsymbol{x},t),\quad \boldsymbol{u}_b(\boldsymbol{x},t)=\boldsymbol{R}\boldsymbol{v}_b(\boldsymbol{R}^{\mathsf{T}}\boldsymbol{x},t)$$

on the swimmer's surface. The surface flow $\boldsymbol{u}_b(\boldsymbol{x},t)$ in the frame of the fluid is derived from $\boldsymbol{v}_b(\boldsymbol{x},t)$ and is also tangential to the surface.

Force and torque on the swimmer. The flow determines the force $\boldsymbol{F}$ and the torque $\boldsymbol{T}$ applied on the swimmer by the fluid via surface integrals of the stress tensor $\boldsymbol{\sigma}$,

$$\frac{\boldsymbol{\sigma}}{\rho}=-p\boldsymbol{I}+\nu[\boldsymbol{\nabla}\boldsymbol{u}+(\boldsymbol{\nabla}\boldsymbol{u})^{\mathsf{T}}],\quad \boldsymbol{F}=\int_S\boldsymbol{\sigma}\hat{\boldsymbol{r}}\,dS,\quad \boldsymbol{T}=\int_S\boldsymbol{r}\times\boldsymbol{\sigma}\hat{\boldsymbol{r}}\,dS,$$

where $\boldsymbol{I}$ is the identity matrix, the superscript T stands for the transpose, dS is an infinitesimal element of the swimmer's surface S, and $\hat{\boldsymbol{r}}$ is the unit vector in the radial direction. We consider the swimmer as a ball having uniform mass density ρ_s neglecting small density changes due to local deformations of the thin surface which represents short cilia or flagella. Thus, the swimmer has mass $m_s=4\pi\rho_s a^3/3$ and constant moment of inertia $J=2m_s a^2/5$. For simplicity, the effects of displacement of the center of mass from the sphere's center (i.e., bottom heaviness; see, e.g., [26]) are not considered here. We have

$$m_s\frac{d\boldsymbol{v}}{dt}=\boldsymbol{F}+(m_s-m_F)\boldsymbol{g},\quad J\frac{d\boldsymbol{\Omega}}{dt}=\boldsymbol{T}, \tag{3}$$

where $\boldsymbol{g}$ is the gravity acceleration and $m_F = 4\pi a^3\rho/3$ is the fluid mass displaced by the sphere. We construct the flow which solves Eq. (2) as a superposition $\boldsymbol{u} = \boldsymbol{u}^s + \boldsymbol{u}^r$ of the flow $\boldsymbol{u}^s$ for an inertialess swimmer in inertial fluid and the flow $\boldsymbol{u}^r$ for a rigid sphere. The former obeys

$$\begin{aligned} &\rho\partial_t\boldsymbol{u}^s = -\boldsymbol{\nabla}p^s + \eta\nabla^2\boldsymbol{u}^s, \quad \boldsymbol{\nabla}\cdot\boldsymbol{u}^s = 0, \quad \boldsymbol{u}^s(\infty) = 0, \\ &\boldsymbol{u}^s(S) = \boldsymbol{v}^s(t) + \boldsymbol{\Omega}^s(t)\times\boldsymbol{x} + \boldsymbol{u}_b(\boldsymbol{x},t), \quad \boldsymbol{F}^s = \boldsymbol{T}^s = 0. \end{aligned} \tag{4}$$

The flow $\boldsymbol{u}^r$ is the flow around a rigid sphere that moves with prescribed translational and angular velocities $\boldsymbol{v} - \boldsymbol{v}^s(t)$ and $\boldsymbol{\Omega} - \boldsymbol{\Omega}^s$, respectively. Thus, it obeys

$$\begin{aligned} &\rho\partial_t\boldsymbol{u}^r = -\boldsymbol{\nabla}p^r + \eta\nabla^2\boldsymbol{u}^r, \quad \boldsymbol{\nabla}\cdot\boldsymbol{u}^r = 0, \quad \boldsymbol{u}^r(\infty) = 0, \\ &\boldsymbol{u}^r(S) = \boldsymbol{v}(t) - \boldsymbol{v}^s(t) + [\boldsymbol{\Omega}(t) - \boldsymbol{\Omega}^s(t)]\times\boldsymbol{x}. \end{aligned} \tag{5}$$

Since $\boldsymbol{u}^s$ imposes zero force and torque on the swimmer, $\boldsymbol{F}$ and $\boldsymbol{T}$ are determined by $\boldsymbol{u}^r$. The force $\boldsymbol{F}(t)$ is the force [22,24] acting on a rigid sphere that moves with velocity $\boldsymbol{v}(t) - \boldsymbol{v}^s(t)$. This is given by the Fourier representation

$$\begin{aligned} &\boldsymbol{F}(t) = -6\pi\eta a\int_{-\infty}^{\infty} f(\delta - i\omega\tau_d)[\hat{\boldsymbol{v}}(\omega) - \hat{\boldsymbol{v}}^s(\omega)]e^{-i\omega t}d\omega, \\ &f(\lambda) = 1 + 3\sqrt{\lambda} + \lambda, \quad \tau_d = \frac{a^2}{9\nu}, \end{aligned} \tag{6}$$

where δ is infinitesimal, so $\sqrt{\delta - i\omega} = \sqrt{|\omega|/2}(1 - i\omega/|\omega|)$. We designate Fourier transforms in time by circumflexes. Similarly, the torque $\boldsymbol{T}$ is given by [24]

$$\begin{aligned} &\boldsymbol{T}(t) = -\int_{-\infty}^{\infty} T_0(\omega)[\hat{\boldsymbol{\Omega}}(\omega) - \hat{\boldsymbol{\Omega}}^s(\omega)]e^{-i\omega t}d\omega, \\ &T_0(\omega) = \frac{5J}{3\gamma\tau_d}\left(1 - \frac{3i\omega\tau_d}{1 + q(\omega\tau_d)}\right), \quad q(\omega) = 3\sqrt{\delta - i\omega}, \end{aligned} \tag{7}$$

where $\gamma = \rho_s/\rho$ is the specific gravity. Thus the force and the torque are determined by $\boldsymbol{v}^s$ and $\boldsymbol{\Omega}^s$, respectively. This way of solution helps separate the effects caused by the inclusion of the inertia of the fluid and of the swimmer.

III. INERTIALESS SWIMMING IN INERTIAL FLUID

In this section we derive translational and rotational velocities attained by an inertialess swimmer in inertial fluid. We circumvent finding $\boldsymbol{u}^s$ by using the reciprocal theorem [16,17,23,29,30]

$$\hat{\boldsymbol{v}}^s\cdot\int_S\hat{\boldsymbol{\sigma}}^k\hat{\boldsymbol{r}}\,dS + a\epsilon_{irn}\hat{\Omega}^s_r\int_S\hat{\sigma}^k_{il}\hat{r}_l\hat{r}_n dS = -\int_S\hat{\boldsymbol{u}}_s\hat{\boldsymbol{\sigma}}^k\hat{\boldsymbol{r}}\,dS, \tag{8}$$

where $\boldsymbol{\sigma}^k$ is the stress tensor of dual flow $\boldsymbol{u}^k$ also obeying unsteady Stokes equations. We use different dual flows for finding the translational and the rotational velocities.

A. Translational velocity

The dual flow, used for finding the translational velocity of the swimmer, is the solution of unsteady Stokes equations whose Laplace transform obeys on the sphere $\hat{u}^k_i = \delta_{ik}$ and decays at infinity. In time domain the flow $\boldsymbol{u}^k$ describes the motion of the sphere that starts from rest at $t = 0$ and has impulsive velocity $u^k_i(|\boldsymbol{x}| = a, t) = \delta(t)\delta_{ik}$ (we do not keep dimensions here since the corresponding dimensional factors disappear from the final formulas). Thus, at $t < 0$ there is no flow and then the velocity jump at $t = 0$ creates a flow. At $t > 0$ the sphere is fixed at the origin and the flow caused by the initial impulse decays. The Fourier transform is readily inferred from the

Laplace transform provided in [23] (see also [31]). We have, on the surface of the sphere,

$$\frac{\hat{\sigma}^k_{il}\hat{r}_l}{3\eta} = \frac{ia\omega\hat{r}_i\hat{r}_k}{6\nu} - \frac{\delta_{ik}(1+q(\omega\tau_d))}{2a}, \tag{9}$$

with $q(\omega)$ defined in Eq. (7). We find, using this flow in Eq. (8), that

$$\hat{\boldsymbol{v}}^s = \left(1 + \frac{i\omega\tau_d}{f(\delta - i\omega\tau_d)}\right)\hat{\boldsymbol{v}}^s_0, \tag{10}$$

where $\boldsymbol{v}^s_0$ is the velocity of the inertialess swimmer in inertialess fluid [29], which using the definitions in Eq. (2) reads

$$\boldsymbol{v}^s_0(t) = -\int_S \boldsymbol{u}_s(\boldsymbol{x},t)\frac{dS}{4\pi a^2} = -\boldsymbol{R}\int_S \boldsymbol{v}_b(\boldsymbol{x},t)\frac{dS}{4\pi a^2}. \tag{11}$$

The inverse Fourier transform of Eq. (10) gives

$$\boldsymbol{v}^s(t) = \boldsymbol{v}^s_0(t) - \frac{d}{dt}\int_{-\infty}^{t} K\left(\frac{t-t'}{\tau_d}\right)\boldsymbol{v}^s_0(t')dt', \tag{12}$$

where we have introduced

$$K(t) = \int \frac{\exp(-i\omega t)}{f(\delta - i\omega)}\frac{d\omega}{2\pi}. \tag{13}$$

We used above that

$$\int \frac{i\omega\tau_d\hat{\boldsymbol{v}}^s_0\exp(-i\omega t)}{f(\delta - i\omega\tau_d)}\frac{d\omega}{2\pi} = -\frac{d}{dt}\int K\left(\frac{t-t'}{\tau_d}\right)\boldsymbol{v}^s_0(t')dt'. \tag{14}$$

We demonstrate that the behavior of $K(t)$ is quite different from that of the $t^{-1/2}$ memory kernel of the force on a rigid sphere [21–24].

B. Memory kernel

We derive the memory kernel $K(t)$ in Eq. (12). We observe that $f^{-1}(z)$ is analytic in the complex plane with a branch cut at the negative real semiaxis. Consequently, $f^{-1}(\delta - i\omega)$, considered as a function of the complex variable ω, is analytic outside the branch cut at $(-i\infty, -i\delta)$. We find $K(t) = 0$ for $t < 0$ because the integration contour can be closed in the upper half plane producing zero. This is necessary for causality; otherwise the instantaneous velocity in Eq. (12) would be determined by future movements of the swimmer. When $t > 0$ we find, passing in Eq. (13) to the integration variable $\lambda = \delta - i\omega$, that

$$K(t) = \int \frac{\exp(-i\omega t)}{f(\delta - i\omega)}\frac{d\omega}{2\pi} = \int_{\delta - i\infty}^{\delta + i\infty}\frac{\exp(\lambda t)}{f(\lambda)}\frac{d\lambda}{2\pi i}, \tag{15}$$

that is, $K(t)$ is the inverse Laplace transform of $1/f(\lambda)$. This conclusion could be reached directly using the Laplace transform instead of the Fourier transform in the derivations. However, this change would have other disadvantages. For use in the next section we consider the slightly more general inverse Laplace transform

$$\tilde{K}(t) = \int_{\delta - i\infty}^{\delta + i\infty}\frac{\exp(\lambda t)}{\tilde{f}(\lambda)}\frac{d\lambda}{2\pi i}, \quad \tilde{f}(\lambda) = 1 + 3\sqrt{\lambda} + \kappa\lambda. \tag{16}$$

The kernel $K(t)$ is obtained from $\tilde{K}(t)$ by setting $\kappa = 1$. We use that

$$\frac{1}{1 + 3\sqrt{\lambda} + \kappa\lambda} = \frac{1}{\sqrt{9 - 4\kappa}}\left[\frac{x_2}{\lambda + x_2\sqrt{\lambda}} - \frac{x_1}{\lambda + x_1\sqrt{\lambda}}\right],$$

where $-x_i$ are roots of the quadratic polynomial $1 + 3x + \kappa x^2$,

$$x_1 = \frac{3 - \sqrt{9 - 4\kappa}}{2\kappa}, \quad x_2 = \frac{3 + \sqrt{9 - 4\kappa}}{2\kappa}. \tag{17}$$

We use the known integral (cf. similar calculation in [6])

$$\int_0^\infty \exp\big(-\lambda t + x_i^2 t\big)\mathrm{erfc}(x_i\sqrt{t})dt = \frac{1}{\lambda + x_i\sqrt{\lambda}},$$

where analytic continuation is used to define the error function $\mathrm{erfc}(x)$ for complex x. We conclude that

$$\tilde{K}(t) = \frac{1}{\sqrt{9 - 4\kappa}}\big[x_2 \exp\big(x_2^2 t\big)\mathrm{erfc}(x_2\sqrt{t}) - x_1 \exp\big(x_1^2 t\big)\mathrm{erfc}(x_1\sqrt{t})\big]. \tag{18}$$

This can be represented as the series

$$\tilde{K}(t) = \frac{1}{\sqrt{9 - 4\kappa}}\left[x_2 \exp\big(x_2^2 t\big) - x_1 \exp\big(x_1^2 t\big) + \frac{2x_1^2\sqrt{t}}{\sqrt{\pi}}\sum_{k=0}^{\infty}\frac{(2t)^k x_1^{2k}}{(2k+1)!!} - \frac{2x_2^2\sqrt{t}}{\sqrt{\pi}}\sum_{k=0}^{\infty}\frac{(2t)^k x_2^{2k}}{(2k+1)!!}\right], \tag{19}$$

which is useful at small t. In contrast to the memory kernel for the force on the rigid sphere, which has square root divergence at zero, $\tilde{K}(t)$ has a finite value of $1/\kappa$ at $t = 0$. When t is large we can use

$$\tilde{K}(t) = \frac{1}{\pi\sqrt{9 - 4\kappa}}\left[\sum_{k=0}^{\infty}\frac{(-1)^k\Gamma(k + 3/2)}{t^{k+3/2}x_1^{2(k+1)}} - \sum_{k=0}^{\infty}\frac{(-1)^k\Gamma(k + 3/2)}{t^{k+3/2}x_2^{2(k+1)}}\right]. \tag{20}$$

The leading-order behavior at large times is given by the $k = 0$ term. We find, using $x_1^{-2} - x_2^{-2} = 3\sqrt{9 - 4\kappa}$, that $\tilde{K}(t) \sim 3t^{-3/2}/\sqrt{4\pi}$. This behavior is independent of κ because the leading-order behavior of $\tilde{f}(\lambda)$ at small λ, given by $[1 + 3\sqrt{\lambda}]^{-1}$, is independent of κ. Thus it holds also that $K(t) \sim 3t^{-3/2}/\sqrt{4\pi}$.

In the case of *Volvox* the density of the swimmer is approximately the density of the fluid, $\kappa \approx 3$, so $\sqrt{9 - 4\kappa} \approx i\sqrt{3}$ and x_i are complex conjugates of each other. We find

$$\tilde{K}(t) = \frac{2\mathrm{Im}\big[x_2 \exp\big(x_2^2 t\big)\mathrm{erfc}(x_2\sqrt{t})\big]}{\sqrt{3}}, \quad x_2 = \frac{3 + i\sqrt{3}}{6}. \tag{21}$$

Finally, we find $K(t)$ by setting $\kappa = 1$ above, which gives

$$\begin{aligned} x_2 &= \frac{3 + \sqrt{5}}{2}, \quad x_1 = \frac{3 - \sqrt{5}}{2}, \\ K(t) &= \frac{1}{\sqrt{5}}\big[x_2 \exp\big(x_2^2 t\big)\mathrm{erfc}(x_2\sqrt{t}) - x_1 \exp\big(x_1^2 t\big)\mathrm{erfc}(x_1\sqrt{t})\big], \end{aligned} \tag{22}$$

with the corresponding asymptotic forms and series. We see that, in contrast with the $t^{-1/2}$ memory kernel for the force that diverges at zero, $K(0)$ is finite and equals one. Moreover, $K(t)$ is integrable due to the $K(t) \sim 3t^{-3/2}/\sqrt{4\pi}$ behavior at large times. We have $\int_0^\infty K(t)dt = 1/f(\lambda = 0) = 1$. Thus $K(t)$ is similar to a δ function smeared over a scale of order one. The integral in Eq. (12) is determined by $|t - t'| \lesssim \tau_d$, where τ_d is defined in Eq. (6). If $\mathrm{Ro} \equiv \sigma\tau_d \ll 1$ then τ_d is much smaller than the swimming period $2\pi/\sigma$ and we can set $\boldsymbol{v}_0^s(t') \approx \boldsymbol{v}_0^s(t)$ in the integrand. We find the leading-order correction in the fluid inertia $\boldsymbol{v}^s = \boldsymbol{v}_0^s - \tau_d d\boldsymbol{v}_0^s/dt$. The correction is small, which is consistent with the negligibility of the time-derivative term in the NSE at $\mathrm{Ro} \ll 1$.

C. Rotational velocity

The dual flow which we use in Eq. (8) to find the rotational velocity of the swimmer is the solution of unsteady Stokes equations whose Laplace transform obeys on the sphere $\hat{u}_i^k = \epsilon_{ikn}x_n$ and decays at infinity. This is flow which is created by instantaneous rotation of the sphere at $t = 0$ with angular velocity given by the unit vector in the kth direction: $u_i^k(x = a, t) = \epsilon_{ikn}x_n\delta(t)$. This flow can be obtained as a superposition of flows caused by rotation of the sphere at an angular velocity that depends on time as $\exp[-i\omega t]$, found in [24]. We find [$y = |\boldsymbol{x}|/a$ and $q = q(\omega\tau_d)$]

$$u_i^k(\boldsymbol{x}, t) = \frac{\epsilon_{ikn}x_n}{y^3}\int \frac{d\omega}{2\pi}\exp[-i\omega t - q(y-1)]\frac{1+qy}{1+q}. \tag{23}$$

If we use spherical coordinates with a polar axis in the kth direction then velocity has the only the nonvanishing component $u_\phi = v$, where [24]

$$v = \frac{x\sin\theta}{y^3}\int \frac{d\omega}{2\pi}\exp[-i\omega t - q(y-1)]\frac{1+qy}{1+q}. \tag{24}$$

The only nonzero component of $\sigma_{il}^k\hat{x}_l$ on the surface S is [24]

$$\begin{aligned}\frac{\sigma_{\phi r}^k}{\eta} &= \left(\frac{\partial v}{\partial x} - \frac{v}{x}\right)\Big|_S = -\sin\theta\left(3\delta(t) + \int \frac{q^2 d\omega}{2\pi(1+q)}e^{-i\omega t}\right),\\ \frac{\hat{\sigma}_{il}^k\hat{x}_l}{\eta} &= -\epsilon_{ikl}\hat{x}_l\left[3 + \frac{q^2}{1+q}\right],\end{aligned} \tag{25}$$

where the second of Eqs. (25) is written in the form independent of the reference frame. We find, using this in Eq. (8), that

$$\boldsymbol{\Omega}^s(t) = -\int_S \frac{3\boldsymbol{x}\times\boldsymbol{u}_s(\boldsymbol{x}, t)dS}{8\pi a^4} = -\boldsymbol{R}\int_S \frac{3\boldsymbol{x}\times\boldsymbol{v}_b(\boldsymbol{x}, t)dS}{8\pi a^4}. \tag{26}$$

This formula is identical to the formula for rotational swimming velocity at zero inertia [29], which has a remarkable consequence, as explained below.

D. Irrelevance of fluid inertia for mean velocity and the scallop theorem

The above formulas imply that the mean swimming velocity of an inertialess swimmer in inertial fluid does not differ at all from the mean velocity of an inertialess swimmer in inertialess fluid. Indeed, we observe that the last term in Eq. (12) is the time derivative of a bounded function. Thus it gives no contribution to the time-averaged velocity. In other words, the time-averaged velocity obeys

$$\langle\boldsymbol{v}^s\rangle = -\frac{1}{4\pi a^2}\left\langle\boldsymbol{R}\int_S \boldsymbol{v}_b(\boldsymbol{x}, t)dS\right\rangle, \tag{27}$$

where the angular brackets stand for the time average [cf. with $\hat{\boldsymbol{v}}^s(\omega = 0) = \hat{\boldsymbol{v}}_0^s(\omega = 0)$ in Eq. (10)]. However, the angular velocity is the same as at zero fluid inertia [see Eq. (26)]. Thus $\boldsymbol{R}$ and surface-averaged $-\boldsymbol{R}\boldsymbol{v}_b$ for inertial fluid do not differ from those for inertialess fluid. The mean swimming velocity is independent of the fluid inertia as long as $\boldsymbol{v}_b$ can be considered as given.

We conclude that the fluid inertia adds only oscillatory motions that produce no net propulsion but can be relevant for nutrient uptake [17]. Correspondingly, the scallop theorem stating that net propulsion is impossible for time-reversible strokes when neglecting the inertia both of the fluid and of the swimmer [18] can be extended to include the fluid inertia. This is in agreement with concrete calculations of [6,16,17].

IV. INCLUDING INERTIA OF THE SWIMMER

We now also incorporate the inertia of the swimmer. We found $\boldsymbol{v}^s$ and thus we can write the force in Eq. (3) which would reproduce the equation of motion derived in [17]. The derivation here provides different insight into the structure of the flow around the swimmer. Our use of this equation is completely different from its use in [17] described previously.

A. Translational velocity with inertia

It is simpler to find the solution directly in Fourier space. Performing a Fourier transform of Eq. (3) and using Eq. (6), we obtain

$$-i\omega\hat{\boldsymbol{v}} = -\frac{f(\delta - i\omega\tau_d)[\hat{\boldsymbol{v}} - \hat{\boldsymbol{v}}^s]}{2\gamma\tau_d} + \frac{2\pi\delta(\omega)(\gamma-1)\boldsymbol{g}}{\gamma}, \tag{28}$$

where we used that initial conditions on velocity in the remote past are forgotten. We obtain the swimmer's velocity by solving for $\hat{\boldsymbol{v}}$ and introducing $\kappa = 1 + 2\gamma$,

$$\hat{\boldsymbol{v}}(\omega) = \left(1 + \frac{i\kappa\omega\tau_d}{\tilde{f}(\delta - i\omega\tau_d)}\right)\hat{\boldsymbol{v}}_0^s + 4\pi\delta(\omega)(\gamma-1)\boldsymbol{g}\tau_d, \tag{29}$$

with $\tilde{f}$ defined in Eq. (16) and where the last term is sedimentation velocity. We find, using similarity to Eqs. (10)–(12),

$$\boldsymbol{v}(t) = \boldsymbol{v}_0^s(t) - \kappa\frac{d\boldsymbol{x}_i(t)}{dt} + 2(\gamma-1)\boldsymbol{g}\tau_d, \tag{30}$$

where we have introduced the inertial displacement $\boldsymbol{x}_i(t)$,

$$\boldsymbol{x}_i = \int_{-\infty}^{t} \tilde{K}\left(\frac{t-t'}{\tau_d}\right)\boldsymbol{v}_0^s(t')dt', \tag{31}$$

with $\tilde{K}$ from Eq. (16). The propulsion velocity given by Eqs. (30) and (31) reduces to that for the inertialess swimmer in Eqs. (10)–(12) by taking $\gamma \to 0$ and $\kappa \to 1$. This is because $K(t)$ is $\tilde{K}(t)$ at $\kappa = 1$. For *Volvox* $\gamma \approx 1$ (see [3]) and $\kappa \approx 3$, so inertia of the swimmer causes a finite change of the swimmer's velocity.

We demonstrated in the preceding section that $\tilde{K}(t)$ is roughly a δ function smeared over $t \sim 1$. Thus we find, by performing consideration similar to that after Eq. (12),

$$\boldsymbol{v} \approx \boldsymbol{v}_0^s - \kappa\tau_d\frac{d\boldsymbol{v}_0^s}{dt}, \quad \mathrm{Ro} \ll 1. \tag{32}$$

The inertial displacement $\boldsymbol{x}_{in}(t)$ is bounded and does not contribute the time-averaged velocity

$$\langle\boldsymbol{v}\rangle = -\frac{1}{4\pi a^2}\left\langle \boldsymbol{R}\int_S \boldsymbol{v}_b(\boldsymbol{x},t)dS\right\rangle + 2(\gamma-1)\boldsymbol{g}\tau_d, \tag{33}$$

where we used Eqs. (11) and (30). This has the same form as the average velocity of an inertialess swimmer in inertialess fluid [29]. This also agrees with the average velocity of the inertialess swimmer in inertialess fluid given by Eq. (27) with sedimentation velocity included. Thus inertia can result in a difference only by changing the rotation matrix $\boldsymbol{R}$. This has a useful consequence, as explained below.

B. Irrelevance of inertia for mean speed at axial symmetry

The case of axially symmetric squirmers is much studied and evokes separate interest. In this case the vectors of translational and angular velocities are parallel, so the swimmer propagates as a screw (see [10] for an example). Then $\boldsymbol{R}$ has no effect in Eq. (33) and can be dropped. The classical swimming theory neglecting inertia applies to the average velocity. We conclude that inertial axially symmetric tangential squirmers obey the scallop theorem as was observed in [6,16,17].

C. Metachronal wave

We consider the metachronal wave as an example of axially symmetric swimming. This stroke is believed to describe *Volvox* with a good approximation [10]. Similarly to [29], we consider only the tangential part described by the time t position of the polar angle θ as a function of the position θ_0 near which the oscillation occurs as $\theta(t,\theta_0)=\theta_0+\epsilon\cos(k\theta_0-\sigma t)$. Our consideration disregards radial and azimuthal displacements. The parameters that fit experiment are $k=4.7$, $\sigma=203$ rad/s, and $\epsilon\approx 0.06$ (see details in [10]). For this stroke there is no rotation and the stroke has only a θ component $v_{b\theta}(t,\theta=\theta(t,\theta_0))=a\partial_t\theta(t,\theta_0)$ [cf. Eq. (1)]. We have to order ϵ such that $\theta_0=\theta(t,\theta_0)-\epsilon\cos\left(k\theta(t,\theta_0)-\sigma t\right)$, which on taking the derivative gives

$$v_{b\theta}(t,\theta)\approx a\sigma\epsilon\sin[k\theta-\sigma t-k\epsilon\cos(k\theta-\sigma t)], \tag{34}$$

which neglects terms of order ϵ^3 and higher. Expanding Eq. (34) in the same order,

$$v_{b\theta}(t,\theta,\phi)\approx a\sigma\epsilon\sin(k\theta-\sigma t)-ak\sigma\epsilon^2\cos^2(k\theta-\sigma t). \tag{35}$$

The axial symmetry dictates that $\boldsymbol{v}_0^s(t)$ points in the vertical direction. We obtain, designating this component by $v_0^s(t)$ and using $v_{bz}=-v_{b\theta}\sin\theta$, that

$$v_0^s(t)=\frac{1}{2}\int_0^\pi v_{b\theta}\sin^2\theta d\theta=\frac{1}{4}\int_0^\pi v_{b\theta}[1-\cos(2\theta)]d\theta.$$

We find, using Eq. (35) and the integrals

$$\int_0^\pi \sin(k\theta-\sigma t)\sin^2\theta\, d\theta=\frac{4\sin(\pi k/2)\sin(\pi k/2-\sigma t)}{k(4-k^2)},$$
$$\int_0^\pi \cos^2(k\theta-\sigma t)\sin^2\theta\, d\theta=\frac{\pi}{4}+\frac{\sin(\pi k)\cos(\pi k-2\sigma t)}{4k(1-k^2)},$$

that the swimming velocity neglecting inertia obeys

$$v_0^s(t)=a\sigma\epsilon\left(\frac{2\sin(\pi k/2)\sin(\pi k/2-\sigma t)}{k(4-k^2)}-\frac{\pi k\epsilon}{8}-\frac{\epsilon\sin(\pi k)\cos(\pi k-2\sigma t)}{8(1-k^2)}\right), \tag{36}$$

up to order ϵ^2. The time average is determined by the only term which does not oscillate $\langle v_0^s(t)\rangle=-\pi a\sigma k\epsilon^2/8$, reproducing result of [29].

We now consider the inertial corrections. We have, by a Fourier transform of Eq. (36),

$$\frac{\hat{v}_0^s}{a\sigma\epsilon\tilde{f}(\delta-i\omega\tau_d)}=\frac{2i\pi\sin(\pi k/2)}{k(4-k^2)}\left(\frac{\exp(-i\pi k/2)\delta(\omega+\sigma)}{\tilde{f}(\delta+i\sigma\tau_d)}-\frac{\exp(i\pi k/2)\delta(\omega-\sigma)}{\tilde{f}(\delta-i\sigma\tau_d)}\right)$$
$$-\frac{\pi\epsilon\sin(\pi k)}{8(1-k^2)}\left(\frac{\exp(i\pi k/2)\delta(\omega-\sigma)}{\tilde{f}(\delta-i\sigma\tau_d)}+\frac{\exp(-i\pi k/2)\delta(\omega+\sigma)}{\tilde{f}(\delta+i\sigma\tau_d)}\right), \tag{37}$$

where we did not write the $\delta(\omega)$ term which does not contribute to the correction. We observe that

$$\tilde{f}(\delta\pm i\sigma\tau_d)=1\pm\frac{i\kappa\,\mathrm{Ro}}{9}+\sqrt{\frac{\mathrm{Ro}}{2}}(1\pm i), \tag{38}$$

so $\tilde{f}(\delta+i\sigma\tau_d)$ and $\tilde{f}(\delta-i\sigma\tau_d)$ are complex conjugates. Using Eq. (29) and performing an inverse Fourier transform of Eq. (37), we find the formula for velocity including inertia of both the fluid and the swimmer

$$\boldsymbol{v}(t)=\boldsymbol{v}_0^s(t)+2(\gamma-1)\boldsymbol{g}\tau_d-a\epsilon\kappa\,\mathrm{Ro}\frac{d}{dt}\left(\frac{2\sin(\pi k/2)}{k(4-k^2)}\right.$$
$$\left.\times\,\mathrm{Im}\left[\frac{\exp(i\pi k/2-i\sigma t)}{\tilde{f}(\delta-iRo)}\right]-\mathrm{Re}\left[\frac{\epsilon\sin(\pi k)\exp(i\pi k/2-i\sigma t)}{8(1-k^2)\tilde{f}(\delta-iRo)}\right]\right), \tag{39}$$

where Im and Re stand for the imaginary and real parts, respectively. It can be concluded that inertia does not change the time-average value of $\boldsymbol{v}(t)$ for this stroke, whereas oscillations of $\boldsymbol{v}(t)$ contain an inertial correction (cf. [17]).

D. Rotational velocity with inertia

The rotational velocity of an inertial swimmer obeys $J\dot{\boldsymbol{\Omega}} = \boldsymbol{T}$. The Fourier transform gives

$$\hat{\boldsymbol{\Omega}}(\omega) = \hat{\boldsymbol{\Omega}}^s(\omega) + \frac{iJ\omega\hat{\boldsymbol{\Omega}}^s(\omega)}{T_0(\omega) - iJ\omega} = \frac{\hat{\boldsymbol{\Omega}}^s(\omega)}{1 - iJ\omega T_0^{-1}(\omega)}, \tag{40}$$

where we used Eq. (7). This solves for the swimmer's rotation implicitly with $\boldsymbol{\Omega}^s$ from Eq. (26). In the time domain,

$$\boldsymbol{\Omega}(t) = \boldsymbol{\Omega}^s(t) - \frac{d}{dt}\int_{-\infty}^{t} K_r\left(\frac{t-t'}{\tau_d}\right)\boldsymbol{\Omega}^s(t')dt', \tag{41}$$

where, using Eq. (7), we have introduced the kernel

$$K_r(t) = \int_{-\infty}^{\infty}\frac{d\omega}{2\pi}\frac{\exp(-i\omega t)}{5\{1 - 3i\omega/[1+q(\omega)]\}/3\gamma - i\omega}. \tag{42}$$

We assume that $5/3\gamma \sim 1$, so this equation gives that the characteristic time of variations of $K_r(t)$ is $O(1)$. We observe that $\int_0^\infty K_r(t)dt$ is finite and given by the Fourier transform at zero frequency, which is $3\gamma/5$. We conclude that $K_r(t)$ decays over time of order one. In the limit of small Roshko number in the leading order we can set $\boldsymbol{\Omega}^s(t') \approx \boldsymbol{\Omega}^s(t)$ in the integrand, finding

$$\boldsymbol{\Omega}(t) \approx \boldsymbol{\Omega}^s(t) - \frac{3\tau_s}{10}\frac{d\boldsymbol{\Omega}^s(t)}{dt}, \quad \mathrm{Ro} \ll 1, \tag{43}$$

where $\tau_s = 2\gamma\tau_d$ is the Stokes time. This formula describes smaller organisms.

E. Inertia changes mean swimming speed via translation-rotation coupling

The inertia of the swimmer, in contrast with the fluid inertia, changes the rotation of the swimmer. Thus, generally, inertia changes $\boldsymbol{R}$ and the net propulsion velocity. This translational-rotational coupling can produce qualitative and quantitative changes in the swimming.

The changes can be considered using Eqs. (30) and (41) describing the propagation of an inertial swimmer in the inertial fluid. Rotation decouples from translation and can be considered separately. In contrast, translation depends on rotation via the rotation matrix $\boldsymbol{R}$ obeying $\dot{R}_{ij} = \epsilon_{ikl}\Omega_k R_{lj}$ [see, e.g., Eq. (33)]. The system of Eqs. (30) and (41) describing the translation-rotation coupling is nonlocal in time, having memory described by the kernels $\tilde{K}(t)$ and $K_r(t)$. It becomes local in the limit of small inertia $\mathrm{Ro} \ll 1$ [see Eqs. (32) and (43)]. Another limit where the equations become local is that of heavy swimmers whose density is much higher than that of the fluid, $\gamma \gg 1$, as explained below.

F. Heavy swimmers

We consider the limit of heavy (called dense in [16]) swimmers whose density is much higher than the density of the fluid, $\gamma \gg 1$. In this limit $\kappa \approx 2\gamma \to \infty$ and we can neglect $3\sqrt{\lambda}$ in $\tilde{f}(\lambda) = 1 + 3\sqrt{\lambda} + \kappa\lambda$ [we observe that we cannot neglect the first term in $\tilde{f}(\lambda)$ that is relevant at $\lambda \lesssim 1/\kappa$]. Thus Eq. (29) becomes

$$\hat{\boldsymbol{v}}(\omega) = \frac{\hat{\boldsymbol{v}}_0^s}{1 - i\omega\tau_s} + 2\pi\delta(\omega)\boldsymbol{g}\tau_s, \tag{44}$$

where we observed that in this limit $\kappa\tau_d$ is the Stokes time $\tau_s = 2\gamma\tau_d$. An inverse Fourier transform gives

$$\frac{d\boldsymbol{v}}{dt} = -\frac{\boldsymbol{v} - \boldsymbol{v}_0^s}{\tau_s} + \boldsymbol{g}. \tag{45}$$

This reproduces the equation for heavy spherical swimmers derived in [16]. The limit of small inertia $\sigma\tau_s \ll 1$ is found by writing $\boldsymbol{v} = \boldsymbol{v}_0^s - \tau_s\dot{\boldsymbol{v}} + \boldsymbol{g}\tau_s$ and making the first iteration of the right-hand side

$$\boldsymbol{v} \approx \boldsymbol{v}_0^s - \tau_s\frac{d\boldsymbol{v}_0^s}{dt} + \boldsymbol{g}\tau_s. \tag{46}$$

This agrees with Eq. (32). Similar consideration holds for the angular velocity. We have, from Eq. (40),

$$\hat{\boldsymbol{\Omega}}(\omega) = \frac{\hat{\boldsymbol{\Omega}}^s(\omega)}{1 - (3i\omega\gamma\tau_d/5)\{1 - 3i\omega\tau_d/[1 + q(\omega\tau_d)]\}^{-1}}, \tag{47}$$

where we have used the definition of $T_0(\omega)$ in Eq. (7). We observe that in the limit of high γ the characteristic frequency ω_c that defines the inverse Fourier transform of $\hat{\boldsymbol{\Omega}}(\omega)$ obeys $\omega_c\tau_d \sim \gamma^{-1}$. This is obtained by the demand that the prefactor in the denominator is of order one. We find, by observing that at these frequencies $\{1 - 3i\omega\tau_d/[1 + q(\omega\tau_d)]\}^{-1} \approx 1$, that

$$\hat{\boldsymbol{\Omega}}(\omega) \approx \frac{\hat{\boldsymbol{\Omega}}^s(\omega)}{1 - 3i\omega\tau_s/10}, \tag{48}$$

where we have used $2\gamma\tau_d = \tau_s$. Performing an inverse Fourier transform,

$$\frac{d\boldsymbol{\Omega}}{dt} = -\frac{10(\boldsymbol{\Omega} - \boldsymbol{\Omega}^s)}{3\tau_s}. \tag{49}$$

We find, by combining the above system of equations on coupled translational and rotational degrees of freedom,

$$\begin{aligned} \tau_s\frac{d\boldsymbol{v}}{dt} + \boldsymbol{v} &= -\frac{1}{4\pi a^2}\boldsymbol{R}\int \boldsymbol{v}_b(\boldsymbol{x}, t)dS, \\ \frac{dR_{il}}{dt} &= \epsilon_{\mathrm{ins}}\Omega_n R_{sl}, \\ \frac{3\tau_s}{10}\frac{d\boldsymbol{\Omega}}{dt} + \boldsymbol{\Omega} &= -\frac{3}{8\pi a^4}\boldsymbol{R}\int \boldsymbol{x}\times\boldsymbol{v}_b(\boldsymbol{x}, t)dS. \end{aligned} \tag{50}$$

This system was obtained in [16] from steady Stokes equations. Setting $\tau_s = 0$ recovers the often-used formulation of Stone and Samuel [29], where inertia of the fluid and the swimmer is neglected [29]. In this case the reciprocal theorem holds, showing that if the swimming stroke is time reversible then no net self-propulsion occurs over the stroke's period. The limit of small inertia $\sigma\tau_s \ll 1$ for rotational velocity is found by writing $\boldsymbol{\Omega} = \boldsymbol{\Omega}^s - 3\tau_s\dot{\boldsymbol{\Omega}}/10$ and making the first iteration of the right-hand side. This reproduces Eq. (43).

V. TRANSLATIONAL-ROTATIONAL COUPLING AT SMALL INERTIA

In this section we analyze the previously derived equations of motion at small Roshko number. We demonstrate that the leading-order correction in Ro to the mean swimming velocity is proportional to the cross product of translational and rotational swimming velocities at $\mathrm{Ro} = 0$. Thus the swimming velocity is given via the swimming stroke $\boldsymbol{v}_b(\boldsymbol{x}, t)$. Our starting point is Eqs. (32) and (43),

$$\boldsymbol{v} = \boldsymbol{v}_0^s - \kappa\tau_d\frac{d\boldsymbol{v}_0^s}{dt}, \quad \boldsymbol{\Omega}(t) = \boldsymbol{\Omega}^s(t) - \frac{3\tau_s}{10}\frac{d\boldsymbol{\Omega}^s(t)}{dt}. \tag{51}$$

These velocities depend on inertia directly through the corrections linear in Ro $\propto \tau_d$ and indirectly through the rotation matrix [see Eq. (11)]. We use, to study the rotation matrix, that

$$\frac{dR_{ij}}{dt} = R_{il}\epsilon_{lpj}\Omega^b_p, \quad \boldsymbol{\Omega}^b = \boldsymbol{R}^{\mathsf{T}}\boldsymbol{\Omega}(t), \tag{52}$$

where we have introduced angular velocity in the body-fixed frame $\boldsymbol{\Omega}^b$, with $\boldsymbol{R}^{\mathsf{T}}$ the matrix transpose of $\boldsymbol{R}$. This equation can be obtained from $\dot{R}_{ij} = \epsilon_{ikl}\Omega_k R_{lj}$ using the rotational invariance of the Levi-Cività tensor, which implies that $\epsilon_{tpj} = \epsilon_{ikl}R_{it}R_{kp}R_{lj}$ for any orthogonal $\boldsymbol{R}$. Indeed, this identity gives $R_{qt}\epsilon_{tpj} = \epsilon_{qkl}R_{kp}R_{lj}$, and using this in $\dot{R}_{ij} = \epsilon_{ikl}R_{kp}R_{lj}\Omega^b_p$ results in Eq. (52). We find, using Eqs. (26) and (51), that in linear order in Ro,

$$\boldsymbol{\Omega}^b = -\int_S \frac{3\boldsymbol{r}\times\boldsymbol{v}_b(\boldsymbol{r},t)dS}{8\pi a^4} + \frac{3\gamma\tau_d}{5}\frac{d}{dt}\int_S \frac{3\boldsymbol{r}\times\boldsymbol{v}_b(\boldsymbol{r},t)dS}{8\pi a^4} + \frac{3\gamma\tau_d}{5}\boldsymbol{\Omega}^b \times \left(\int_S \frac{3\boldsymbol{r}\times\boldsymbol{v}_b(\boldsymbol{r},t)dS}{8\pi a^4}\right), \tag{53}$$

where we have used $\boldsymbol{R}^{\mathsf{T}}(\boldsymbol{\Omega}\times\boldsymbol{\Omega}^s) = \boldsymbol{\Omega}^b \times (\boldsymbol{R}^{\mathsf{T}}\boldsymbol{\Omega}^s)$. Iterating this equation (which contains $\boldsymbol{\Omega}^b$ on both sides), we find that in linear order in Ro the last term can be dropped,

$$\boldsymbol{\Omega}^b = -\int_S \frac{3\boldsymbol{r}\times\boldsymbol{v}_b(\boldsymbol{r},t)dS}{8\pi a^4} + \frac{3\tau_s}{10}\frac{d}{dt}\int_S \frac{3\boldsymbol{r}\times\boldsymbol{v}_b(\boldsymbol{r},t)dS}{8\pi a^4}. \tag{54}$$

Thus, $\boldsymbol{\Omega}^b$, in contrast with $\boldsymbol{\Omega}$, is completely determined by $\boldsymbol{v}_b(\boldsymbol{x},t)$ and is independent of $\boldsymbol{R}$. This is why we use it to find $\boldsymbol{R}$ in Eq. (52). We rewrite the equation as

$$\frac{d\boldsymbol{R}}{dt} = \boldsymbol{R}\left(\boldsymbol{W} - \frac{3\tau_s}{10}\frac{d\boldsymbol{W}}{dt}\right), \tag{55}$$

where we have introduced the antisymmetric matrix W such that

$$W_{lj} = -\epsilon_{lpj}\left(\int_S \frac{3\boldsymbol{r}\times\boldsymbol{v}_b(\boldsymbol{r},t)dS}{8\pi a^4}\right)_p. \tag{56}$$

We look for the solution of Eq. (55) to linear order in Ro. The zeroth-order solution $\boldsymbol{R}_0$ obeys $\dot{\boldsymbol{R}}_0 = \boldsymbol{R}_0\boldsymbol{W}$. We look for a solution in the form $\boldsymbol{R} = (1+\delta\boldsymbol{R})\boldsymbol{R}_0$, where $\delta\boldsymbol{R} \propto$ Ro. We have

$$\frac{d\delta\boldsymbol{R}}{dt} = -\frac{3\tau_s}{10}\boldsymbol{R}_0\frac{d\boldsymbol{W}}{dt}\boldsymbol{R}_0^{\mathsf{T}} = -\frac{3\tau_s}{10}\frac{d}{dt}\big[\boldsymbol{R}_0\boldsymbol{W}\boldsymbol{R}_0^{\mathsf{T}}\big], \tag{57}$$

where we observed that

$$\frac{d}{dt}\big[\boldsymbol{R}_0\boldsymbol{W}\boldsymbol{R}_0^{\mathsf{T}}\big] = \boldsymbol{R}_0\frac{d\boldsymbol{W}}{dt}\boldsymbol{R}_0^{\mathsf{T}}, \tag{58}$$

which is readily verified using antisymmetry $\boldsymbol{W}^{\mathsf{T}} = -\boldsymbol{W}$. We conclude, by integrating Eq. (57) from 0 to t with $\delta\boldsymbol{R}(0) = 0$ [implied by $R_{ij}(0) = \delta_{ij}$], that

$$\delta\boldsymbol{R} = -\frac{3\tau_s}{10}\boldsymbol{R}_0[\boldsymbol{W}(t) - \boldsymbol{W}(0)]\boldsymbol{R}_0^{\mathsf{T}}. \tag{59}$$

We observe that $\delta\boldsymbol{R}$ is an antisymmetric matrix as it must be by the orthogonality of $\boldsymbol{R}$. We can write, using Eq. (56),

$$\delta R_{ik} = \frac{3\tau_s}{10}(R_0)_{il}(R_0)_{kj}\epsilon_{lpj}\left(\int_S \frac{3\boldsymbol{r}\times[\boldsymbol{v}_b(\boldsymbol{r},t) - \boldsymbol{v}_b(\boldsymbol{r},t=0)]dS}{8\pi a^4}\right)_p, \tag{60}$$

which gives, using $(R_0)_{rp}\epsilon_{rki} = (R_0)_{il}(R_0)_{kj}\epsilon_{lpj}$, that

$$\delta R_{ik} = \frac{3\tau_s}{10}\epsilon_{ikr}\big[\Omega^{ss}_r(t) - \Omega^{ss}_r(0)\big]. \tag{61}$$

We introduced the Stone-Samuel angular velocity of an inertialess swimmer in inertialess fluid

$$\boldsymbol{\Omega}^{ss}(t) = -\boldsymbol{R}_0 \int_S \frac{3\boldsymbol{r} \times \boldsymbol{v}_b(\boldsymbol{r}, t) dS}{8\pi a^4}. \tag{62}$$

We find the swimmer's velocity using this rotation matrix from Eqs. (11) and (51),

$$\boldsymbol{v} = \boldsymbol{v}^{ss} - \kappa \tau_d \frac{d\boldsymbol{v}^{ss}}{dt} + \frac{3\tau_s}{10} \boldsymbol{v}^{ss} \times [\boldsymbol{\Omega}^{ss}(t) - \boldsymbol{\Omega}^{ss}(0)], \tag{63}$$

where we have used Eq. (61) and introduced the Stone-Samuel velocity of an inertialess swimmer in inertialess fluid [29]

$$\boldsymbol{v}^{ss} = -\boldsymbol{R}_0 \int_S \boldsymbol{v}_b(\boldsymbol{x}, t) \frac{dS}{4\pi a^2}. \tag{64}$$

The velocities $\boldsymbol{v}^{ss}$ and $\boldsymbol{\Omega}^{ss}$ are $\boldsymbol{v}_0^s$ and $\boldsymbol{\Omega}^s$ in Eqs. (11) and (26) with rotational matrix $\boldsymbol{R}$ obtained neglecting the inertia. The appearance of $\boldsymbol{\Omega}^{ss}(0)$ is not because of infinite memory but rather because the rotation matrix that transforms velocities from the body-fixed frame to the fluid frame has a reference orientation at $t = 0$. Thus, the leading-order correction to the swimming velocity in inertia of both the fluid and the swimmer is derived simply from the zeroth-order velocities, obtained neglecting the inertia. For a time-reversible stroke the scallop theorem [18] guarantees that $\langle \boldsymbol{v}^{ss} \rangle = 0$ so that the average velocity $\langle \boldsymbol{v} \rangle_{tr}$ of a swimmer with time-reversible stroke obeys

$$\langle \boldsymbol{v} \rangle_{tr} = \frac{3\tau_s}{10} \langle \boldsymbol{v}^{ss} \times \boldsymbol{\Omega}^{ss} \rangle + o(\mathrm{Ro}). \tag{65}$$

The right-hand side is nonzero for an asymmetric stroke, demonstrating the breakdown of the scallop theorem due to inertia. We stress that this is the leading-order result in Ro, which does not imply that time-reversible strokes for which $\boldsymbol{v}^{ss}$ and $\boldsymbol{\Omega}^{ss}$ are parallel cannot swim by inertia. In fact, these strokes can be relevant for *Volvox* and nonzero swimming velocity can appear in higher-order terms.

We observe that Eqs. (63) and (65) hold also for heavy swimmers with $\sigma \tau_s \ll 1$. Thus we conclude that in this case the scallop theorem breaks down. In contrast, [16] claimed that the scallop theorem holds also for heavy swimmers with a time-reversible tangential stroke. This is because they did not consider the rotational-translational coupling for this system.

VI. SWIMMING AT ARBITRARY INERTIA UNDER A TIME-REVERSIBLE STROKE

The observations made in the preceding section persist to higher Ro. We illustrate this by considering swimming due to the general asymmetric stroke given by

$$\theta(t, \theta_0, \phi_0) = \theta_0 + \epsilon y(\sigma t) + c\epsilon h(\phi_0) y(\sigma t), \tag{66}$$

where $h(\phi_0)$ and $y(\sigma t)$ are some functions, c is a constant, and ϵ represents the small amplitude of this type of cilia motion. Below the results of general calculations will be evaluated numerically for $h(\phi_0) = \cos(\phi_0)$ and $y(\sigma t) = \cos(\sigma t)$, where the stroke becomes

$$\theta(t, \theta_0, \phi_0) = \theta_0 + \epsilon \cos(\sigma t) + c\epsilon \cos(\phi_0) \cos(\sigma t). \tag{67}$$

Importantly, the last term induces asymmetry that causes oscillatory rotation in the $\hat{\boldsymbol{y}}$ direction, which in turn gives nonzero net displacement. Qualitatively, equal strength time-reversible rowers are located along each longitude and the strength of the rowers depends on the azimuthal angle ϕ (see Fig. 1).

We demonstrate below that the results obtained for any asymmetry function $h(\phi_0)$ do not differ from those for $h(\phi_0) = \cos\phi_0$. In contrast, the use of different $y(t)$ can give quantitatively (but not qualitatively) different answers. We consider the nongravitational component of velocity and include gravity later.

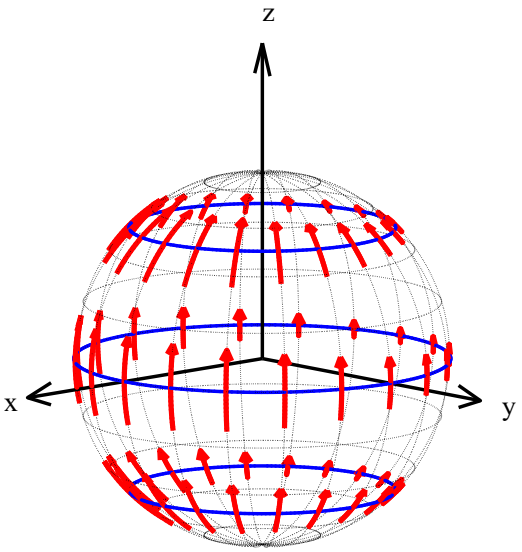

FIG. 1. Illustration of the asymmetric stroke in Eq. (67) on a sphere. The arrows denote oscillation amplitudes of the tangential velocity distribution which are directed along longitudes and vary with ϕ along latitudes. For $c = 0$, the swimmer only oscillates in pure translation along the symmetry axis z. For $c \neq 0$ there is an additional oscillatory rotation about the y axis due to asymmetry and the inertial rotation-translation coupling generates nonzero net translation along the x axis.

The asymmetry function $h(\phi_0)$ describes how different the motion of cilia at different azimuthal angles is. It is a periodic function with period 2π and zero average whose Fourier series is

$$h(\phi_0) = \sum_{n=1}^{\infty} [a_n \cos(n\phi_0) + b_n \sin(n\phi_0)]. \tag{68}$$

We define constant c in Eq. (66) so that $a_1^2 + b_1^2 = 1$. We assume that the modulation is of order one, so c is also of order one. The function y characterizes a periodic swimming stroke and has the Fourier series representation

$$y(\sigma t) = \sum_{n=1}^{\infty} [c_n \cos(n\sigma t) + d_n \sin(n\sigma t)], \tag{69}$$

so σ is the swimming stroke frequency. For motion given by Eq. (66) the swimming stroke $\boldsymbol{v}_b$ has only a θ component given by $v_{b\theta}(\theta, \phi) = a\epsilon\sigma[1 + h(\phi)c]y'(\sigma t)$. Thus,

$$\begin{aligned} v_{bz} &= -a\epsilon\sigma[1 + h(\phi)c]y'(\sigma t)\sin\theta, \\ v_{bx} &= a\epsilon\sigma[1 + h(\phi)c]y'(\sigma t)\cos\phi\cos\theta, \\ v_{by} &= a\epsilon\sigma[1 + h(\phi)c]y'(\sigma t)\sin\phi\cos\theta. \end{aligned} \tag{70}$$

It is then found that

$$\begin{aligned} \boldsymbol{v}_s &\equiv -\int_S \boldsymbol{v}_b(\boldsymbol{x}, t)\frac{dS}{4\pi a^2} = \frac{\pi}{4}a\epsilon\sigma y'(\sigma t)\hat{\boldsymbol{z}}, \\ \hat{\boldsymbol{p}} &= a_1\hat{\boldsymbol{y}} - b_1\hat{\boldsymbol{x}}, \\ \boldsymbol{\Omega}_s &\equiv -\int_S \frac{3\boldsymbol{r}\times\boldsymbol{v}_b(\boldsymbol{r}, t)dS}{8\pi a^4} = -\frac{3c\epsilon\sigma y'(\sigma t)}{4}\hat{\boldsymbol{p}}, \end{aligned} \tag{71}$$

where a_1 and b_1 are defined in Eq. (68). We observe that $\hat{\boldsymbol{p}}$ is a unit vector aligned with the constant rotation axis in the x-y plane. Using the reference frame rotated in the plane so that the $\hat{\boldsymbol{p}}$ has only a y component, we find

$$\boldsymbol{v}_s = \frac{\pi}{4} a\epsilon\sigma y'(\sigma t)\hat{\boldsymbol{z}}, \quad \boldsymbol{\Omega}_s = -\frac{3c\epsilon\sigma y'(\sigma t)}{4}\hat{\boldsymbol{y}}, \tag{72}$$

which is identical to what we would obtain using $h(\phi_0) = \cos(\phi_0)$ in Eq. (66).

We start from considering the case of $\mathrm{Ro} \ll 1$ where Eq. (65) holds. We observe that

$$\boldsymbol{v}^{ss} \times \boldsymbol{\Omega}^{ss} = \boldsymbol{R}_0(\boldsymbol{v}_s \times \boldsymbol{\Omega}_s) = \frac{3\pi ac\epsilon^2\sigma^2[y'(\sigma t)]^2}{16}\boldsymbol{R}_0\hat{\boldsymbol{x}}. \tag{73}$$

In the leading order in ϵ the matrix $\boldsymbol{R}_0$ is a unit matrix since $\Omega_s \propto \epsilon$. We find, from Eq. (65),

$$\langle \boldsymbol{v}\rangle_{tr} = \frac{9\pi ac\epsilon^2\sigma^2\gamma\tau_d}{80}\langle [y'(\sigma t)]^2\rangle\hat{\boldsymbol{x}}. \tag{74}$$

This gives, for the stroke given by Eq. (67) with $y(\sigma t) = \cos(\sigma t)$, that

$$\langle \boldsymbol{v}\rangle_{tr} = \frac{\pi ac\epsilon^2\sigma\gamma\alpha^2}{80}\hat{\boldsymbol{x}}, \tag{75}$$

where we have defined $\alpha^2 = 9\sigma\tau_d/2$. Returning to the case of arbitrary Ro, we have, from Eq. (40), that

$$\hat{\boldsymbol{\Omega}}(\omega) = \frac{(\boldsymbol{R}\boldsymbol{\Omega}_s)(\omega)}{1 - iJ\omega T_0^{-1}(\omega)} = -\frac{3c\epsilon\sigma}{4}\frac{[y'(\sigma t)\boldsymbol{R}\hat{\boldsymbol{y}}](\omega)}{1 - iJ\omega T_0^{-1}(\omega)}, \tag{76}$$

where in this formula we designate the Fourier transform of some function $q(t)$ by $(q)(\omega)$. We observe that since the rotation is around the y axis $\boldsymbol{R}\hat{\boldsymbol{y}} = \hat{\boldsymbol{y}}$. We find

$$\hat{\boldsymbol{\Omega}}(\omega) = \frac{3i\pi c\epsilon\omega\hat{\boldsymbol{y}}}{4}\sum_{n=1}^{\infty}\left(\frac{c_n[\delta(\omega + n\sigma) + \delta(\omega - n\sigma)]}{1 - iJ\omega T_0^{-1}(\omega)} - \frac{id_n[\delta(\omega + n\sigma) - \delta(\omega - n\sigma)]}{1 - iJ\omega T_0^{-1}(\omega)}\right), \tag{77}$$

where we have used Eq. (69). The inverse Fourier transform gives

$$\boldsymbol{\Omega}(t) = \frac{3c\epsilon\sigma\hat{\boldsymbol{y}}}{4}\sum_{n=1}^{\infty}\left[nc_n\mathrm{Im}\left(\frac{\exp(in\sigma t)}{1 + iJn\sigma T_0^{-1}(-n\sigma)}\right) - nd_n\mathrm{Re}\left(\frac{\exp(in\sigma t)}{1 + iJn\sigma T_0^{-1}(-n\sigma)}\right)\right], \tag{78}$$

where we have used $T_0(-\omega) = T_0^*(-\omega)$. Introducing the rotation angle $\psi(t) = \int_0^t \Omega(t')dt'$, we find

$$\psi(t) = \frac{3c\epsilon}{4}\sum_{n=1}^{\infty}\left[c_n\mathrm{Re}\left(\frac{1 - \exp(in\sigma t)}{1 + iJn\sigma T_0^{-1}(-n\sigma)}\right) + d_n\mathrm{Im}\left(\frac{1 - \exp(in\sigma t)}{1 + iJn\sigma T_0^{-1}(-n\sigma)}\right)\right]. \tag{79}$$

We have that, up to quadratic order in ϵ,

$$\boldsymbol{R}(t)\boldsymbol{v}_s(t) = \frac{\pi}{4}a\epsilon\sigma y'(\sigma t)\psi(t)\hat{\boldsymbol{x}} + O(\epsilon^3). \tag{80}$$

We find for the time-average velocity, using that it equals the time average of $\boldsymbol{R}(t)\boldsymbol{v}_s(t)$ giving $\langle \boldsymbol{v}\rangle = \pi a\epsilon\sigma\langle y'(\sigma t)\psi(t)\rangle\hat{\boldsymbol{x}}/4$, that

$$\langle \boldsymbol{v}\rangle = -\frac{3\pi ca\epsilon^2\sigma\hat{\boldsymbol{x}}}{16}\sum_{n=1}^{\infty}\left(c_n\mathrm{Re}\left\langle\frac{\exp(in\sigma t)y'(\sigma t)}{1 + iJn\sigma T_0^{-1}(-n\sigma)}\right\rangle + d_n\mathrm{Im}\left\langle\frac{\exp(in\sigma t)y'(\sigma t)}{1 + iJn\sigma T_0^{-1}(-n\sigma)}\right\rangle\right).$$

We find, performing the time averaging,

$$\langle \boldsymbol{v} \rangle = \frac{3\pi c a \epsilon^2 \sigma \hat{\boldsymbol{x}}}{32} \sum_{n=1}^{\infty} \mathrm{Re}\left(\frac{i\left(c_n^2 + d_n^2\right)}{1 + iJn\sigma T_0^{-1}(-n\sigma)} \right). \tag{81}$$

We observe that

$$\mathrm{Re}\left(\frac{i}{1 + iJn\sigma T_0^{-1}(-n\sigma)} \right) = \mathrm{Re}\left[\left(\frac{T_0(-n\sigma)}{Jn\sigma} + i \right)^{-1} \right].$$

We have, from Eq. (7), that

$$\frac{T_0(-n\sigma)}{Jn\sigma} = \frac{15}{2\gamma\alpha_n^2} + \frac{5i}{\gamma(1 + \alpha_n + i\alpha_n)}, \tag{82}$$

where we introduced $\alpha_n = 3\sqrt{n\,\mathrm{Ro}/2}$. We find

$$\begin{aligned} \langle \boldsymbol{v} \rangle &= U_0 a \sigma \hat{\boldsymbol{x}} + 2(\gamma - 1)\boldsymbol{g}\tau_d, \\ U_0 &= \frac{3\pi c \epsilon^2}{32} \sum_{n=1}^{\infty} \left(c_n^2 + d_n^2\right) \mathrm{Re}\left[\left(\frac{15}{2\gamma\alpha_n^2} + i + \frac{5i}{\gamma(1 + \alpha_n + i\alpha_n)} \right)^{-1} \right], \end{aligned} \tag{83}$$

where we introduced the velocity U_0 that determines displacement in body sizes per stroke and included the sedimentation velocity due to gravity. The corresponding formula for the case of Eq. (67) is obtained by setting all c_n and d_n to zero except for $c_1 = 1$, which gives

$$U = \frac{3\pi c \epsilon^2}{32} \mathrm{Re}\left[\left(\frac{15}{2\gamma\alpha^2} + i + \frac{5i}{\gamma(1 + \alpha + i\alpha)} \right)^{-1} \right], \tag{84}$$

with $\alpha = 3\sqrt{\mathrm{Ro}/2}$ defined after Eq. (75). This formula reproduces Eq. (75) in the small-Roshko-number limit. We study U as a function of the free parameters of the swimming stroke γ, σ, and a. Writing Eq. (84) explicitly as a real-valued function gives

$$U = \left| \frac{15}{2\gamma\alpha^2} + \frac{5\alpha}{\gamma(1 + 2\alpha + 2\alpha^2)} + i + \frac{5i(1 + \alpha)}{\gamma(1 + 2\alpha + 2\alpha^2)} \right|^{-2} \frac{3\pi c \epsilon^2}{32} \left(\frac{15}{2\gamma\alpha^2} + \frac{5\alpha}{\gamma(1 + 2\alpha + 2\alpha^2)} \right).$$

We find that dimensionless velocity factorizes as

$$U = \frac{3\pi c \epsilon^2}{32} \tilde{U}(\gamma, \alpha), \tag{85}$$

where the dimensionless function $\tilde{U}$ of two dimensionless numbers γ and α is

$$\tilde{U} = \gamma(1 + 2\alpha + 2\alpha^2)[15(1 + 1/\alpha + 1/2\alpha^2) + 5\alpha]/D, \tag{86}$$

with the denominator D,

$$D = [15(1 + 1/\alpha + 1/2\alpha^2) + 5\alpha]^2 + [\gamma(1 + 2\alpha + 2\alpha^2) + 5(1 + \alpha)]^2. \tag{87}$$

Figure 2 shows a log-log plot of U as a function of Roshko number Ro for $\gamma = 1$, where sedimentation velocity vanishes. Interestingly, the speed U vanishes at the limits $\mathrm{Ro} \to \{0, \infty\}$ and attains a maximum at an intermediate value of $\mathrm{Ro} \approx 2.8$ (vanishing at $\mathrm{Ro} \to 0$ is due to the scallop theorem [18] and at $\mathrm{Ro} \to \infty$ due to large mass). This can be interpreted either as an optimal flapping frequency σ or as an optimal body radius a for a fixed frequency. Remarkably, setting physical values of $\sigma = 200$ rad/s and $\nu = 10^{-6}$ m^2/s for *Volvox* in water gives an optimal radius of $a \approx 355$ μm, which falls well within the size range of large *Volvox* colonies [3].

We also observe that the dependence on the density of the swimmer has the form $U(\gamma) = \gamma/(b_2\gamma^2 + b_1\gamma + b_0)$, where b_i are functions of Ro only. The corresponding definitions of b_i can

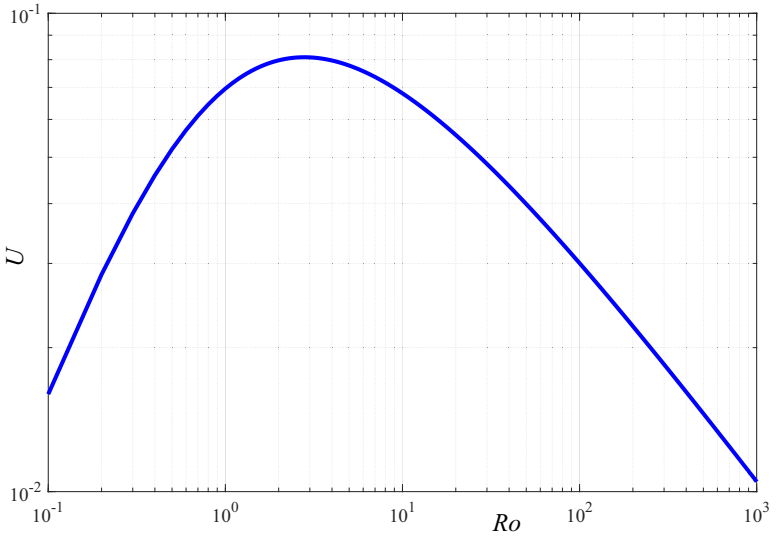

FIG. 2. A log-log plot of nondimensional speed U as a function of Roshko number Ro. The maximum is reached at Ro ≈ 2.8.

be readily obtained from Eq. (86). Elementary calculus of $U'(\gamma) = 0$ gives that U, considered as a function of the density of the swimmer, has a maximum at an optimal density ratio of

$$\gamma^* = \frac{5\sqrt{(3/2\alpha^2 + 3/\alpha + 3 + \alpha)^2 + (1+\alpha)^2}}{1 + 2\alpha + 2\alpha^2}. \tag{88}$$

While for physical values of *Volvox* the optimal value is $\gamma \sim 10$, this value results in a high sedimentation velocity in Eq. (33), which can hardly be overcome by the strokes. Therefore, *Volvox* typically tend to a density ratio of nearly neutral buoyancy ($\gamma = 1.003$; cf. [3]) for which sedimentation is nonzero yet small and the above optimum has fewer implications.

We consider Eq. (84) at size in the range 100–500 μm that is typical for *Volvox* and at fixed σ (the period of flagella motion depends weakly on the size). We find that the dimensionless swimming velocity depends on the dimensionless parameters of the stroke as ϵ^2 times an order one constant c times a numerical factor. This type of parametric dependence is quite universal. For instance, for the stroke $\theta = \theta_0 + \epsilon\cos(n\theta_0 - \omega t)$ considered in [29] we have $U \propto n\epsilon^2$. The same stroke combined with small radial deformations is considered to model *Volvox* (see, e.g., [10]). The radial deformations do not cause a strong change in the parametric dependence: We have $U \propto \epsilon^2$ with the proportionality coefficient depending on n and the ratio of amplitudes of angular and radial motions. We conclude that the flapping stroke prescribed by Eq. (66) generates a swimming velocity that is quite similar to that for irreversible strokes. This is of course because inertia is of order one Ro ~ 1, so the scallop theorem's breakdown is of order one. Since the radial displacements would probably not destroy the phenomenon, this way of self-propulsion could be used by *Volvox* to reach velocities similar to those achieved by irreversible strokes. This way of swimming, if realized, could be done during turns toward or away from external stimuli such as light in phototaxis [13,26]. It might also occur in emergency cell swimming similar to the escape of *Paramecia* from a heat source where a time-reversible stroke was observed [25,32]. Whether this type of swimming is really used by *Volvox* or other microswimmers for the actual motion is to be decided by future observations from experimental measurements.

VII. SUMMARY AND DISCUSSION

We have studied the motion of inertial squirmers using the unsteady Stokes equation. Using the reciprocal theorem, we derived the swimmer's translation and rotation under any given stroke of tangential deformation. Our analysis extends the well-known work [29] of Stone and Samuel from the inertialess to the inertial case. It also generalizes previous works on inertial squirmers [17] which considered only axisymmetric strokes where rotation is either zero or decoupled from translation [10]. As a consequence, we showed that an asymmetric time-reversible stroke can lead to net propulsion through dynamic coupling between rotation and translation. For small inertia this coupling is described by the vector product of inertialess translational and rotational velocities. If the product has a nonzero time average, then the net propulsion velocity is finite even for a time-reversible stroke. For a model of the asymmetric stroke, the normalized swimming speed is maximized for intermediate values of an $O(1)$ Roshko number which falls well within the realistic range of large *Volvox* colonies. For $\mathrm{Ro} \to 0$, our results reduce to those of the inertialess swimmer in [29]. For $\mathrm{Ro} \to \infty$, U decays as $1/\sqrt{\mathrm{Ro}}$. We conjecture that swimming optimization at $\mathrm{Ro} \sim 1$ can be one of the reasons for the cutoff in size of *Volvox* colonies at $a \approx 500\ \mu$m [3].

We now briefly discuss some limitations of our work and suggest possible directions for future extension. Our current work is limited to tangential strokes, whereas *Volvox* strokes involve also a radial component, which must be included in future extensions of the analysis for a realistic description. For axisymmetric strokes, time-reversible deformation with nonzero radial component can lead to net propulsion of inertial squirmers [6,16]. Nevertheless, inclusion of the radial stroke seemingly would not destroy the asymmetric swimming mechanism displayed here. Indeed, considering surface deformations as a sum of radial and tangential displacements, we would find the sum of the corresponding contributions also in the swimming velocity. The velocity would include also the terms due to the coupling of radial and tangential deformations. There seems to be no reason why the terms involving radial displacements would cancel the terms due to tangential displacements, destroying the effect described here. Of course only the complete calculation can fully prove this point, which is left as an open challenge. Also left for future work is the comparison of the two mechanisms of swimming (our mechanism and axisymmetric time-reversible deformation with nonzero radial component) using a full solution of the flow in the vicinity of the deforming boundary for general strokes. The general solution will also enable calculation of mechanical energy dissipation, which will give another criterion for stroke optimization.

We did not consider here the effects of bottom heaviness (center-of-mass displacement from the sphere's center). This could produce coupling between rotation, caused by the gravitational torque, and inertial translation similar to that considered in this work. The study of this coupling is of interest and left for future work. Finally, a longer-term goal is to use these improvements to the theoretical model in order to match it with experimental measurements of swimming *Volvox*. This will help in quantifying the true contribution of inertial effects to *Volvox* motion.

Large organisms often use time-reversible strokes for swimming while small ones do not, since they obey the scallop theorem [18]. When inertia becomes not completely negligible the time-reversible stroke becomes a possible way of swimming and it can be used as in the case of *Paramecia* [25,32]. It seems of interest to study how the efficiency of the time-reversible stroke improves with growing inertia of the organisms and for which the time-reversible stroke becomes advantageous. Our work provides a step in this direction of study.

Our main discovery in this work is that the spherical squirmer model contains strokes in which swimming can occur by inertial coupling of rotation and translation. In this context the following question arises: Is the spherical squirmer model, possibly with inclusion of the most general small deformations of the shape and the effects of inertia, able to shed light on the reasons for the rotation of *Volvox* in nature? Currently, the only attempt at incorporation of the *Volvox* rotation in the theory is done with the help of an axisymmetric (independent of the azimuthal angle) swirl [10]. In this frame rotation and translation are uncoupled, leaving the reasons for rotation unclear. The authors of [10] proposed that the modeling of *Volvox* interaction with the fluid by a continuous boundary

whose shape is fully controlled by the swimmer can be invalid. In fact, our work demonstrates that not all the phenomena that can be captured by the model are exhausted. The possibility of coupling rotation to translation can give new reasons for rotating (as it did in the study of phototaxis [13,26]). Unfortunately, the stroke introduced in this work is currently detached from the data and more fully time-resolved measurements of strokes of real *Volvox* are needed for progress. The challenge of a proper theoretical understanding of *Volvox* rotation remains open and requires further work.

ACKNOWLEDGMENT

This work was supported by the Israel Science Foundation through Grant No. 567/14.

[1] M. J. Lighthill, On the squirming motion of nearly spherical deformable bodies through liquids at very small Reynolds numbers, Commun. Pure Appl. Math. **5**, 109 (1952).
[2] J. R. Blake, A spherical envelope approach to ciliary propulsion, J. Fluid Mech. **46**, 199 (1971).
[3] R. E. Goldstein, Green algae as model organisms for biological fluid dynamics, Annu. Rev. Fluid Mech. **47**, 343 (2015).
[4] T. J. Pedley, Spherical squirmers: Models for swimming micro-organisms, IMA J. Appl. Math. **81**, 488 (2016).
[5] D. R. Brumley, M. Polin, T. J. Pedley, and R. E. Goldstein, Hydrodynamic Synchronization and Metachronal Waves on the Surface of the Colonial Alga *Volvox carteri*, Phys. Rev. Lett. **109**, 268102 (2012).
[6] K. Ishimoto, A spherical squirming swimmer in unsteady Stokes flow, J. Fluid Mech. **723**, 163 (2013).
[7] K. Ishimoto and M. Yamada, A rigorous proof of the scallop theorem and a finite mass effect of a microswimmer, arXiv:1107.5938.
[8] D. R. Brumley, M. Polin, T. J. Pedley, and R. E. Goldstein, Metachronal waves in the flagellar beating of *Volvox* and their hydrodynamic origin, J. R. Soc. Interface **12**, 20141358 (2015).
[9] D. R. Brumley, R. Rusconi, K. Son, and R. Stocker, Flagella, flexibility and flow: Physical processes in microbial ecology, Eur. Phys. J. Spec. Top. **224**, 3119 (2015).
[10] T. J. Pedley, D. R. Brumley, and R. E. Goldstein, Squirmers with swirl: A model for *Volvox* swimming, J. Fluid Mech. **798**, 165 (2016).
[11] D. R. Brumley, K. Y. Wan, M. Polin, and R. E. Goldstein, Flagellar synchronization through direct hydrodynamic interactions, eLife **3**, 02750 (2014).
[12] S. Ghose and R. Adhikari, Irreducible Representations of Oscillatory and Swirling Flows in Active Soft Matter, Phys. Rev. Lett. **112**, 118102 (2014).
[13] O. S. Pak and E. Lauga, Generalized squirming motion of a sphere, J. Eng. Math. **88**, 1 (2014).
[14] B. U. Felderhof, Spinning swimming of volvox by tangential helical wave, arXiv:1601.00755.
[15] B. U. Felderhof and R. B. Jones, Stokesian swimming of a sphere at low Reynolds number by helical surface distortion, Phys. Fluids **28**, 073601 (2016).
[16] D. Gonzalez-Rodriguez and E. Lauga, Reciprocal locomotion of dense swimmers in Stokes flow, J. Phys.: Condens. Matter **21**, 204103 (2009).
[17] S. Wang and A. M. Ardekani, Unsteady swimming of small organisms, J. Fluid Mech. **702**, 286 (2012).
[18] E. M. Purcell, Life at low Reynolds number, Am. J. Phys. **45**, 3 (1977).
[19] A. Shapere and F. Wilczek, Geometry of self-propulsion at low Reynolds number, J. Fluid Mech. **198**, 557 (1989).
[20] E. Lauga, Continuous breakdown of Purcell's scallop theorem with inertia, Phys. Fluids **19**, 061703 (2007).
[21] A. B. Basset, *A Treatise on Hydrodynamics* (Deighton Bell, Cambridge, 1888), Vol. 2.
[22] J. Boussinesq, *Theorie Analytique de la Chaleur* (Gauthiers-Villars, Paris, 1903), Vol. II.

[23] M. R. Maxey and J. J. Riley, Equation of motion for a small rigid sphere in a nonuniform flow, Phys. Fluids **26**, 883 (1983).
[24] L. D. Landau and E. M. Lifshitz, *Fluid Mechanics: Course of Theoretical Physics*, 2nd ed. (Elsevier, Amsterdam, 2009), Vol. 6.
[25] A. Hamel, C. Fisch, L. Combettes, P. Dupuis-Williams, and C. N. Baroud, Transitions between three swimming gaits in *Paramecium* escape, Proc. Natl. Acad. Sci. USA **108**, 7290 (2011).
[26] K. Drescher, R. E. Goldstein, and I. Tuval, Fidelity of adaptive phototaxis, Proc. Natl. Acad. Sci. USA **107**, 11171 (2010).
[27] A. S. Khair and N. G. Chisholm, Expansions at small Reynolds numbers for the locomotion of a spherical squirmer, Phys. Fluids **26**, 011902 (2014).
[28] T. A. Spelman and E. Lauga, Arbitrary axisymmetric steady streaming: Flow, force and propulsion, J. Eng. Math. **105**, 31 (2017).
[29] H. A. Stone and A. D. Samuel, Propulsion of Microorganisms by Surface Distortions, Phys. Rev. Lett. **77**, 4102 (1996).
[30] S. Kim and S. J. Karrila, *Microhydrodynamics: Principles and Selected Applications* (Butterworth-Heinemann, Boston, 1991).
[31] J. M. Burgers, *Second Report on Viscosity and Plasticity* (Nordemann, New York, 1938), p. 113.
[32] E. Lauga, Emergency cell swimming, Proc. Natl. Acad. Sci. USA **108**, 7655 (2011).